Catena 124 (2015) 119–129

Contents lists available at ScienceDirect

Catena

journal homepage: www.elsevier.com/locate/catena

Eolian deposition in the alpine zone of the Uinta Mountains, Utah, USA

Jeffrey S. Munroe *, Emily C. Attwood, Samuel S. O'Keefe, Paul J.M. Quackenbush

Geology Department, Middlebury College, Middlebury, VT 05753, USA

ARTICLE INFO

Article history:
Received 26 May 2014
Received in revised form 3 September 2014
Accepted 14 September 2014
Available online 8 October 2014

Keywords:
Loess
Pedogenesis
Alpine zone
Mineralogy
Geochemistry

ABSTRACT

Field and laboratory investigations were conducted to determine the origin of a ubiquitous layer of silt that caps soil profiles in the alpine zone of the Uinta Mountains, Utah, USA. Fine sediment isolated from snowbanks was studied to constrain the fraction of this material derived from allochthonous eolian additions. Lake sediments representing deposition over the past few centuries were analyzed to determine whether dust deposition in the Uintas has been a long-term process, and if properties of the modern dust differ from dust which accumulated prior to European settlement. Results indicate that alpine soils have been strongly influenced by long-term eolian deposition. The loess cap in these soil profiles averages 18 cm thick, and physical and chemical properties of soil horizons derived from the eolian parent material are significantly different than those of the subsurface horizons derived from in situ produced congelifractate. Fine sediment observed at the surface of snowbanks in the early summer is a mixture of silty exotic eolian material and sandy locally derived sediment. Snowbanks on ridgecrests and on slopes of blocky scree tend to accumulate the maximum amount of exotic dust with the minimum amount of local material. The grain-size distribution, mineralogy, and geochemistry of lake sediments indicate that dust has been accumulating in the Uintas for at least the last few centuries. Modern lake sediments are significantly enriched in elements indicative of upwind mining and agricultural activity, recording an anthropogenic change in dust composition following settlement of the surrounding lowland basins.

1. Introduction

Dust deposition is increasingly recognized as an important process in mountain environments. Dust is generated in lowland regions by a variety of natural and anthropogenic disturbance mechanisms (e.g. Neff et al., 2008; Painter et al., 2007), and can be transported long distances by atmospheric circulation (e.g. Arimoto, 2001; Steenburgh et al., 2012; Vandenberghe, 2013). Upon deposition, dust induces a variety of effects in mountain geoecosystems, including alteration of the hydrologic cycle through snowpack darkening (e.g. Painter et al., 2007, 2010), changes in surface water chemistry (e.g. Brahney et al., 2014; Moser et al., 2010; Psenner, 1999), and contributing to soil formation (e.g. Dahms, 1993; Lawrence et al., 2011).

Recent work in the Rocky Mountains of the western U.S. has considered various aspects of the modern dust system. Some studies have investigated rates of contemporary dust accumulation and reported evidence that these rates changed following European settlement (e.g. Dahms and Rawlins, 1996; Lawrence and Neff, 2009; Lawrence et al., 2010; Neff et al., 2008). A second line of research has focused on the identification of possible dust source regions (e.g. Brahney et al., 2013; Muhs and Benedict, 2006; Neff et al., 2008), including work in dryland systems upwind of the mountains (e.g. Reheis et al., 2009). A third research direction has involved quantifying the impacts of dust deposition on the hydrologic cycle (e.g. Painter et al., 2007, 2010; Steenburgh et al., 2012; Steltzer et al., 2009).

Related to these projects is another group of studies concerned with the impact of dust deposition on soil development, and the utility of soils as recorders of dust deposition over time. In some ways these studies are similar to those focused on pedogenesis in island systems, where dust is an important vector for exotic mineralogies and elemental inputs (e.g. Dia et al., 2006; Dymond et al., 1974; Engelbrecht et al., 2014; Kurtz et al., 2001; Menéndez et al., 2007). In the Rocky Mountains, several projects have presented pedologic and stratigraphic evidence for past dust deposition, and have considered the effects of dust accretion on pedogenesis (e.g. Birkeland et al., 1987; Lawrence et al., 2011, 2013; Litaor, 1987; Thorn and Darmody, 1980). Yet questions remain about the history and operation of dust systems in this region that can only be answered through further field and laboratory analyses of modern dust, mountain soils, and other surficial deposits.

This study focused on dust and alpine soil development in the Uinta Mountains (hereafter, the "Uintas") of northeastern Utah (Fig. 1). The Uintas are a major component of the Rocky Mountain system and contain an expansive area of above-treeline terrain. Much of this landscape has relatively gentle slopes, and as a result the alpine soils are well-developed. These soils have been the target of previous studies (e.g. Bockheim and Koerner, 1997; Bockheim et al., 2000; Munroe, 2007), which revealed that pedons in the Uintas commonly feature a stony sand at depth overlain by a stone-poor fine silt layer at the surface (Fig. 2). It has been proposed that this silt layer, which is present

* Corresponding author. Tel.: +1 802 443 3446: fax: +1 802 443 2072.
E-mail address: jmunroe@middlebury.edu (J.S. Munroe).

http://dx.doi.org/10.1016/j.catena.2014.09.008
0341-8162/

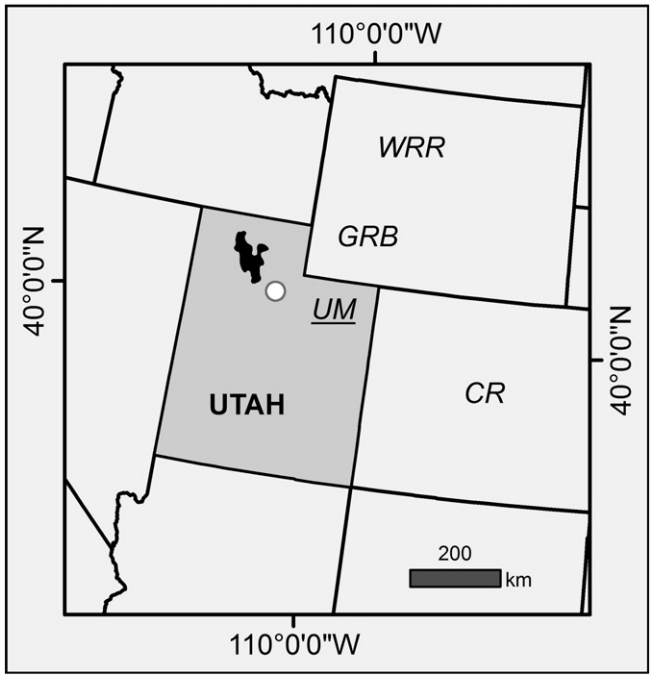

Fig. 1. Location of the Uinta Mountains (UM) in northeastern Utah. The black polygon denotes the Great Salt Lake and the circle marks Salt Lake City. WRR is the Wind River Range in Wyoming, GRB the Green River Basin, and CR the Colorado Rockies.

throughout a wide elevation range and over landforms of varying ages, is an alpine loess deposit (Bockheim and Koerner, 1997; Bockheim et al., 2000). Other studies have noted the circum-neutral pH of surface waters in the Uintas (Christensen and Jewell, 1998), despite the absence of a widespread buffer in the dominantly quartzite bedrock underlying the alpine landscape, raising the possibility that dust deposition plays a role in buffering acidic precipitation. Several recent studies have considered the influence of dust deposition on snowpack albedo in the nearby Wasatch Mountains (e.g. Carling et al., 2012; Reynolds et al., 2013; Steenburgh et al., 2012). Most recently, the grain-size distribution, geochemistry, and mineralogy of modern dust in the Uintas were investigated using passive dust collectors (Munroe, 2014), shedding light on the composition and flux of contemporary dust to the alpine zone; however, no previous study was specifically designed to investigate the role of dust deposition in alpine pedogenesis, the extent of dust in snow, and the history of the dust system in the Uintas. Accordingly, the objectives of this study were:

1. To investigate the degree to which dust deposition has influenced pedogenesis in the extensive Uinta alpine zone;
2. To determine the origin of fine material noted at the surface of late-lying snowbanks in the Uinta alpine zone;
3. To evaluate whether dust deposition in the Uinta alpine zone is a recent process; and
4. To assess whether properties of dust accumulating in the Uinta alpine zone changed following European settlement in the surrounding lowland basins.

Fig. 2. Photograph of a representative soil profile in the alpine zone of the Uinta Mountains. A cap of stone-poor, silty material is clearly visible overlying a coarser subsoil. This surficial layer is interpreted as an alpine loess deposit.

2. Setting

The Uinta Mountains are a major component of the Rocky Mountain system located in northeastern Utah, where they extend for ~200 km along a west-to-east axis into northwestern Colorado (Fig. 1). Maximum elevations are in excess of 4 km, culminating in Kings Peak at 4123 m asl. The Uintas are cored by the Uinta Mountain Group, a thick sequence of upper Precambrian siliciclastic rocks and lightly metamorphosed quartzite, which has been folded into a doubly plunging anticline (Bradley, 1995; Dehler et al., 2007; Sears et al., 1982). The range was extensively glaciated during the Pleistocene, and during the Last Glacial Maximum (~20,000 years ago), glaciers covered a total area of ~2000 km^2 (Munroe and Laabs, 2009). No glaciers remain in the Uintas today, and basal dates from lake sediment cores indicate that the range was essentially ice free by the beginning of the Holocene (Munroe, 2002).

Despite the extent of glaciation during the Pleistocene, the highest elevations of the Uintas were above the reach of alpine glaciers, and the ridgecrest was only locally inundated by erosive ice where glaciers were confluent through low cols. As a result, large areas at high elevations (>3400 m) are dominated by gently sloping summit flats (Munroe, 2006). Bedrock outcrops are rare on these periglacial uplands, which are almost continuously mantled by congelifractate, a regolith of unknown thickness containing grain sizes from silt through coarse boulders (Bradley, 1936). In some places this material forms a smooth mantle, carpeted by tundra vegetation, whereas in other locations the congelifractate has been reworked into periglacial features including sorted polygons up to 10 m in diameter, and sorted stripes up to 3 m wide (Munroe, 2007). These features appear inactive under modern climate conditions, given the degree of lichen cover on stones and the extent of turf cover in polygon centers. In contrast, smaller, non-sorted frost boils, which are common throughout the alpine zone, appear to be actively cryoturbating as evidenced by bare mineral soil.

Information about the climate at high elevations in the Uintas is provided by the Chepeta Remote Automated Weather Station (RAWS) at an elevation of 3700 m. Data captured by this RAWS reveal a mean annual air temperature of −2.0 °C and a mean wind speed of 6.2 m/s. Air temperatures during the summer (June/July/August) average 8.2 °C, whereas winter temperatures (December, January, February) average −10.2 °C. Precipitation is measured at automated Snowpack Telemetry (SNOTEL) stations throughout the Uintas at locations below treeline

(~2400–3300 m). Total annual precipitation at these sites ranges from ~50–100 cm/yr, with roughly half of that accumulating as snow.

3. Methods

This project utilized field and laboratory investigations, along with compilation of existing data, to evaluate the effects and history of eolian deposition in the alpine zone of the Uintas. Samples were collected from locations throughout the Uinta (Table 1). Efforts were focused on four main sediment types: modern dust, soils, fines in snowbanks, and lake sediments.

3.1. Modern dust

Properties and flux of modern dust to the Uinta alpine zone were determined for samples from four passive dust collectors deployed between June 2011 and June 2013 (Table 1). Details about the design of these collectors, and the measured dust properties, are presented in Munroe (2014). Briefly, the collectors are a modified version of the classic marble dust trap (e.g. Sow et al., 2006), measuring 56 × 56 cm, and filled with ~7 kg of black glass beads. Dust is washed from a collector with distilled water, concentrated in the lab through centrifuging, and treated with hydrogen peroxide to remove organic matter before analysis.

3.2. Soils

To characterize soils across the Uinta alpine zone, published and unpublished field descriptions of soil profiles were combined with observations from new locations (Table 1) to generate a database of alpine loess thickness and soil properties. Field descriptions were made of soil profiles exposed in hand-dug pits following standard protocols. Published and unpublished laboratory data on soil chemistry were combined with measurements made on new samples. Measurements including bulk density, electric conductivity, pH, organic C, N, P, Mg, Ca, Na, K, sum of exchangeable bases, base saturation, and cation exchange capacity were made following standard protocols. The majority of these analyses were made at the University of Wyoming soils lab, with the remainder made at the University of Missouri.

3.3. Snowbanks

Fine clastic materials are often observed on the surface of late-lying snowbanks in the Uinta alpine zone. It is unclear, however, whether these fines represent atmospheric dust deposition, or sediment from the surrounding land surface that is transported onto the snowbanks in the spring. In June of 2013, samples of dirty snow were collected from 14 snowbanks in a variety of landscape positions, including nivation hollows, cornices, and ridgecrests (Table 1). Fourteen samples were also collected from the ground surface surrounding these snowbanks and designated as "SNS" for "Soil Near Snow." Dirty snow was collected in acid-washed 1-L Nalgene bottles; SNS samples were collected in ziplock bags. In the lab, snow samples were melted and sediment was isolated from the water by centrifuging.

3.4. Lake sediments

Short (~30 cm) sediment cores were collected from seven lakes (Table 1) in June, 2013 using a UWITEC Complete Corer operated from an inflatable boat. Cores were retrieved from the vicinity of the deepest point in each lake basin, determined through sounding. Cores were sampled on site into plastic bags at three depth intervals: 0–3 cm, 12–15 cm, and 27–30 cm.

3.5. Lab analyses

The combined set of soil, modern dust, snow, SNS, and lake sediment samples was subjected to a consistent suite of laboratory analyses. Grain-size distribution was determined through laser scattering with a Horiba LA-950. This instrument has an effective range of 50 nm to 3 mm, and calculations were made using a refractive index of 1.54, and an imaginary component of 0.1i. Samples were reacted with H_2O_2 to remove organic matter, dispersed using sodium hexametaphosphate, mixed, and sonified before analysis.

Next, samples of soil, SNS, and lake sediment were mechanically dispersed and settled in Atterberg cylinders to isolate the <~20-μm fraction that overlaps with the grain-size distribution of modern dust. Samples of sediment from snowbanks were too small for this treatment; however, their grain-size distributions naturally overlap with the modern dust so they were analyzed in bulk. Oriented slides of all samples were prepared for X-ray diffraction (XRD) analysis using an eyedropper. Mineralogical composition was determined through XRD using a Bruker D-8 diffractometer with CuKα radiation, theta compensating slits, and a graphite monochromator. Each sample was scanned from 2 to 40°, with a step time of 1 s.

Major and trace element geochemistry was evaluated through ICP-MS analysis following a 4-acid digestion at SGS Minerals. Results were reported in % for major elements, and in ppm for trace elements. Bivariate plots of immobile elements were constructed to assess whether the different sediment types were derived from the same source.

Finally, the significance of differences in variables between groups of samples was assessed with a nonparametric Mann Whitney U-test, given the relatively small sample sizes and non-normal distributions. A *P*-value of 0.05 was used as the threshold when assessing statistical significance.

4. Results

4.1. Modern dust

Properties of modern dust accumulating in the alpine zone of the Uintas are described in detail elsewhere (Munroe, 2014), but are briefly summarized here. On the basis of two years of collections, the average dust flux is 3.5 gm/m^2/yr. The dominant grain-size fractions in the dust are very fine silt (31%, 2 to 7 μm) and fine silt (27%, 7 to 14 μm). Eight percent of the dust falls in the clay size fraction (<2 μm). The overall mean grain-size of the dust is 13 μm (6.3 Φ), with a median of 9.1 μm (6.8 Φ). XRD analysis indicates that the dust is dominated by quartz, plagioclase, K-feldspar, and illite with minor amounts of kaolinite, chlorite, and amphibole. Geochemical analysis reveals that Bi, Na, P, Zn, Sn, Cu, Cd, Ba, Ni, W, Sb, Pb, and Tl are present in dust at concentrations 10× to >80× greater than their abundances in local bedrock.

4.2. Soils

A capping layer of surficial silt overlying coarser material was noted in every soil profile in the Uinta alpine zone. On the basis of field measurements at 53 localities, the thickness of this layer averages 18 cm, with a median of 15 and a range of 5 to 34 cm (Fig. 3). The distribution of thicknesses is approximately normal, with a slight positive skewness of 0.4.

Grain-size analysis with a combination of sieving and hydrometer techniques indicates that the abundance of sand is significantly ($P = 0.000$) greater in B horizons (60 vs. 46%), whereas silt is significantly ($P = 0.000$) greater in A horizons (42 vs. 28%, Table 2, Fig. 4). In contrast, the clay content is similar between horizons (~12%, Fig. 4). Analysis with laser scattering (Table 3) reveals that B horizons tend to be coarser than A horizons (32 vs. 19 μm); however, this difference is not significant ($P = 0.470$). Very fine sand and coarse silt are significantly ($P = 0.000$) more abundant in A horizons (median of 9.2 vs.

Table 1
Locations of sample sites in the Uinta Mountains.

Site	Type	Latitude[a]	Longitude[a]	Elevation (m)	Reference
DUST1	Dust	40.81000	−110.07346	3651	Munroe (2014)
DUST2	Dust	40.63793	−110.46607	3400	Munroe (2014)
DUST3	Dust	40.68048	−110.88959	3283	Munroe (2014)
DUST4	Dust	40.82629	−110.49868	3747	Munroe (2014)
GB0501	Soil	40.80422	−110.25122	3495	Munroe (unpublished)
GB0502	Soil	40.80435	−110.25133	3496	Munroe (unpublished)
GB0503	Soil	40.80478	−110.25153	3500	Munroe (unpublished)
GB0504	Soil	40.80513	−110.25015	3510	Munroe (unpublished)
GB0505	Soil	40.80425	−110.25450	3503	Munroe (unpublished)
GB0506	Soil	40.81412	−110.27225	3622	Munroe (unpublished)
GB0507	Soil	40.81852	−110.26908	3697	Munroe (unpublished)
LP0501	Soil	40.76683	−109.84910	3523	Munroe (2007)
LP0502	Soil	40.76635	−109.84988	3525	Munroe (2007)
LP0503	Soil	40.76632	−109.85078	3527	Munroe (2007)
LP0504	Soil	40.76518	−109.85672	3535	Munroe (2007)
LP0505	Soil	40.76513	−109.85565	3534	Munroe (2007)
LP0506	Soil	40.76508	−109.85663	3535	Munroe (2007)
NP0501	Soil	40.79855	−110.11092	3736	Munroe (2007)
NP0502	Soil	40.79813	−110.11160	3735	Munroe (2007)
NP0503	Soil	40.79812	−110.11155	3735	Munroe (2007)
NP0504	Soil	40.79827	−110.11142	3735	Munroe (2007)
NP0505	Soil	40.79810	−110.11057	3735	Munroe (2007)
NP0506	Soil	40.79915	−110.11098	3736	Munroe (2007)
DUST1	Soil	40.81000	−110.07346	3691	This study
DUST2	Soil	40.63793	−110.46607	3410	This study
DUST3	Soil	40.68048	−110.88959	3412	This study
DUST4	Soil	40.82629	−110.49868	3775	This study
BF-98-02	Soil	40.88107	−110.50836	3276	Munroe (unpublished)
U90-2	Soil	40.81390	−109.99644	3665	Bockheim and Koerner (1997)
U90-3	Soil	40.81235	−110.03142	3458	Bockheim and Koerner (1997)
U90-5	Soil	40.76803	−109.87973	3613	Bockheim and Koerner (1997)
U90-6	Soil	40.76714	−109.84695	3521	Bockheim and Koerner (1997)
U92-1	Soil	40.80033	−110.05789	3491	Bockheim and Koerner (1997)
U92-3	Soil	40.78146	−110.10443	3595	Bockheim and Koerner (1997)
U92-4	Soil	40.79653	−110.10543	3706	Bockheim and Koerner (1997)
U92-6	Soil	40.81927	−110.02610	3556	Bockheim and Koerner (1997)
U92-7	Soil	40.81729	−110.04617	3676	Bockheim and Koerner (1997)
U92-8	Soil	40.79700	−109.99498	3447	Bockheim and Koerner (1997)
U97-3	Soil	40.81146	−110.14855	3423	Bockheim et al. (2000)
U97-5	Soil	40.82038	−110.16164	3646	Bockheim et al. (2000)
DUST1-S	Soil	40.81003	−110.07325	3691	This study
DUST1-E	Soil	40.81030	−110.07294	3690	This study
DUST1-W	Soil	40.81028	−110.07366	3690	This study
DUST1-N	Soil	40.81069	−110.07354	3688	This study
DUST1	Soil	40.80997	−110.07345	3691	This study
RAWS	Soil	40.81029	−110.07339	3690	This study
DUST2	Soil	40.63859	−110.46597	3405	This study
DUST2-N	Soil	40.63806	−110.46594	3409	This study
DUST2-W	Soil	40.63800	−110.46603	3409	This study
DUST2-OLD	Soil	40.63793	−110.46609	3410	This study
DUST2-E	Soil	40.63787	−110.46539	3410	This study
DUST2-S	Soil	40.63740	−110.46565	3410	This study
DUST3-W	Soil	40.68047	−110.89180	3415	This study
DUST3-N	Soil	40.68085	−110.89168	3415	This study
DUST3-S	Soil	40.68035	−110.89145	3417	This study
DUST3-E	Soil	40.68075	−110.89068	3418	This study
DUST3	Soil	40.68027	−110.88895	3403	This study
DUST4-A	Soil	40.82633	−110.49833	3773	This study
DUST4-X	Soil	40.82632	−110.49837	3773	This study
DUST4-B	Soil	40.82624	−110.49864	3775	This study
DUST4-C	Soil	40.82618	−110.49908	3776	This study
DUST4-D	Soil	40.82562	−110.50067	3775	This study
DUST4-W	Soil	40.82577	−110.50041	3770	This study
DUST4	Soil	40.82628	−110.49868	3775	This study
ELBOW	Lake sediment	40.79408	−110.04239	3330	This study
HESSIE	Lake sediment	40.86835	−110.42920	3237	This study
HOOVER	Lake sediment	40.67970	−110.87081	3020	This study
MARSHALL	Lake sediment	40.67585	−110.87578	3057	This study
READER	Lake sediment	40.79096	−110.05993	3311	This study
SWASEY	Lake sediment	40.66712	−110.46722	3268	This study
TAYLOR	Lake sediment	40.78681	−110.09191	3421	This study
SNOW01	Snow and SNS	40.79804	−110.10803	3727	This study
SNOW02	Snow and SNS	40.79796	−110.10370	3700	This study
SNOW03	Snow and SNS	40.80050	−110.10041	3657	This study
SNOW04	Snow and SNS	40.80061	−110.09670	3588	This study

Table 1 *(continued)*

Site	Type	Latitude[a]	Longitude[a]	Elevation (m)	Reference
SNOW05	Snow and SNS	40.78510	−109.92305	3502	This study
SNOW06	Snow and SNS	40.79013	−109.92365	3511	This study
SNOW07	Snow and SNS	40.79602	−109.93450	3602	This study
SNOW08	Snow and SNS	40.80778	−109.96856	3702	This study
SNOW09	Snow and SNS	40.64443	−110.45967	3290	This study
SNOW10	Snow and SNS	40.63929	−110.46022	3378	This study
SNOW11	Snow and SNS	40.82550	−110.50032	3782	This study
SNOW12	Snow and SNS	40.83077	−110.49857	3684	This study
SNOW13	Snow and SNS	40.84344	−110.49865	3558	This study
SNOW14	Snow and SNS	40.85515	−110.49718	3482	This study

[a] WGS-84.

5.4%, and 13.0 vs. 8.5% respectively). Differences between A and B soil horizons in the abundances of other grain-size fractions are not significant.

Bulk density, electric conductivity, organic C, N, P, Mg, Ca, Na, K, sum of exchangeable bases, and CEC are significantly different between A and B horizons (Table 2). All of these properties are greater in A horizons except for bulk density, which is greater in B horizons (1.42 vs. 1.13 gm/cm^3). In contrast, pH, C:N, and base saturation are not significantly different between the two horizon groups.

X-ray diffraction analysis reveals that plagioclase and amphibole are present in samples from A horizons (Fig. 5). In contrast, amphibole is not detectable in B horizons, and plagioclase appears less abundant. B horizons are instead dominated by quartz, orthoclase feldspar, and pedogenic clays. Plagioclase and amphibole are also absent in the underlying bedrock.

Geochemical analysis with ICP-MS (Table 4) reveals that A horizons are significantly enriched in Ca ($P = 0.000$), Cd ($P = 0.000$), Cu ($P = 0.013$), and S ($P = 0.001$) relative to B horizons. In contrast, B horizons are significantly enriched in Al ($P = 0.000$), Ce ($P = 0.035$), Fe ($P = 0.004$), La ($P = 0.041$), Th ($P = 0.03$), Ti ($P = 0.001$), Tl ($P = 0.001$), U ($P = 0.015$), V ($P = 0.000$), and Zr ($P = 0.010$). Bivariate plots of immobile elements reveal that A and B horizons are generally similar to each other, although some B horizon samples plot closer to Uinta bedrock (Fig. 6).

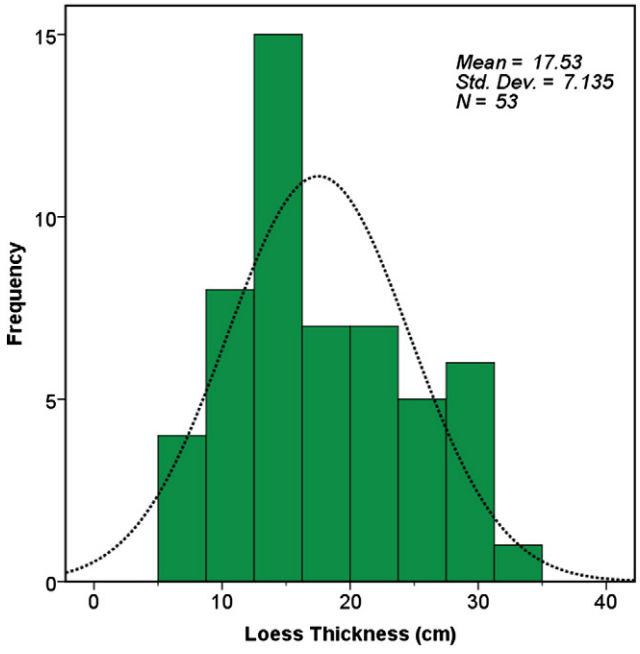

Fig. 3. Distribution of loess thickness measurements from the alpine zone of the Uinta Mountains.

4.3. Snowbanks and Soil Near Snow (SNS)

Grain-size analysis reveals (Fig. 7) that the clastic sediment isolated from late-lying snowbanks is significantly ($P = 0.012$) finer than the ground surface (SNS samples) in the vicinity of the snowbanks (mean of 88.8 vs. 145.7 μm). Coarse sand (4.8 vs. 3.4%, $P = 0.024$), medium sand (20.0 vs. 3.3%, $P = 0.000$), and fine sand (14.7 vs. 7.9%, $P = 0.001$) are significantly more abundant in SNS samples; very fine sand (22.3 vs. 8.8%, $P = 0.000$) and coarse silt (19.1 vs. 11.8%, $P = 0.000$) are significantly more abundant in snow samples. Abundances of <2-μm material, along with medium, fine, and very fine silt, are not significantly different between the two sample types.

Samples of sediment isolated from the snow contain two distinct grain-size modes (Fig. 7): a mode of fine to medium (~10–20 μm) silt (up to 45%), and coarser mode of very fine (~80 μm) sand (up to 38%). A few samples contain a third mode of coarse (~1000 μm) sand (up to 25%). In contrast, the grain-size distribution of SNS samples is coarser than that of most A horizons, with a dominant mode of medium sand, and a secondary mode of fine to medium silt.

X-ray diffraction analysis reveals that both the sediment within the snow, and the SNS samples, contain amphibole and plagioclase (Fig. 5). Neither of these minerals is present in the local bedrock, although both are present in modern dust samples. Geochemically, SNS samples are indistinguishable from other A horizons, and snow samples plot in a tight cluster overlapping with modern dust (Fig. 6).

4.4. Lake sediments

The grain-size distribution of lake sediments is very similar to that of the modern dust (Fig. 7). Overall, lake sediment samples are dominated by very fine silt (22%), and clay (<2-μm, 22%). Very fine silt is also the dominant mode in modern dust samples (30%), although fine silt is the second most abundant grain-size fraction (27%); as noted earlier, clay-sized material makes up ~8% of the modern dust samples.

The overall mean grain-size of the lake sediments is ~10 μm. Cores from the 7 sampled lakes exhibit a variety of down-core trends in grain-size. In two lakes, mean grain-size increases downward; in two others mean grain-size decreases downward, and for three lakes the mean grain-size is essentially constant from top to bottom.

The surface cores were not directly dated; however, ^{210}Pb depth-age models have previously been produced for lakes in the Uintas (e.g. Reynolds et al., 2010 Moser, personal comm.), including two of the lakes in this study. Although sedimentation rates vary somewhat between lakes, overall the depths considered here (~15 cm and ~30) correspond approximately to the beginnings of the 19th and 16th centuries. Thus, the middle and bottom samples in this study likely record sedimentation before European settlement.

X-ray diffraction reveals that the mineralogical composition of lake sediments has been consistent over the past few centuries. Plagioclase is present in all lake sediment samples and modern dust samples, despite the general absence of this mineral in Uinta bedrock, indicating

Table 2
Summary data for soil A and B horizons.

Horizon	Statistic	BD[a] gm/cm^3	pH	EC[b] DS/M	C %	N %	C:N	PO_4-P mg/kg	Exchangeable (meq/100 gm)				Exch. bases meq/100 gm	CEC[c] meq/100 gm	BS[d] %	Sand[e] %	Silt[e] %	Clay[e] %
									Mg	Ca	Na	K						
A	Mean	1.13	5.3	0.6	6.8	0.6	11.9	16.8	2.2	9.4	0.2	0.6	12.3	26.4	53.9	46.1	41.5	12.4
	Median	1.16	5.2	0.5	6.1	0.6	11.4	7.0	1.7	6.4	0.1	0.5	9.0	23.7	56.6	50.4	36.9	10.1
	Max	1.46	6.5	1.9	24.0	1.9	17.7	168.0	7.7	34.0	1.1	2.5	41.9	77.4	100.0	89.0	86.3	59.6
	Min	0.53	4.0	0.1	0.5	0.0	9.6	0.0	0.1	0.4	0.0	0.0	1.0	3.8	5.0	0.0	6.0	1.0
	Skew	−0.46	0.12	0.89	1.35	0.99	1.21	3.49	1.57	1.72	3.25	1.37	1.64	1.05	0.00	−0.39	0.60	2.59
	Count	20	59	42	46	46	46	46	60	60	58	59	60	60	60	97	97	97
B	Mean	1.44	5.2	0.2	0.8	0.1	11.5	3.4	1.1	3.0	0.1	0.3	4.4	9.7	48.2	59.5	28.1	12.0
	Median	1.43	5.2	0.2	0.4	0.0	11.7	1.0	0.8	2.6	0.1	0.2	3.8	8.7	49.5	64.0	22.0	10.9
	Max	1.81	6.9	2.1	6.2	0.6	24.0	26.0	4.3	11.5	0.8	1.7	13.9	29.7	91.8	84.1	88.7	65.0
	Min	0.90	4.0	0.0	0.1	0.0	1.7	0.0	0.1	0.1	0.0	0.0	0.5	1.2	3.0	5.0	12.3	0.0
	Skew	−0.54	0.22	5.39	2.96	2.75	0.06	2.00	1.64	1.14	2.43	2.96	1.17	1.29	−0.30	0.67	0.12	2.23
	Count	32	100	60	87	85	59	85	100	100	95	98	100	100	100	115	115	115

[a] Bulk density.
[b] Electric conductivity.
[c] Cation exchange capacity.
[d] Base saturation.
[e] Determined by sieving and hydrometer analysis.

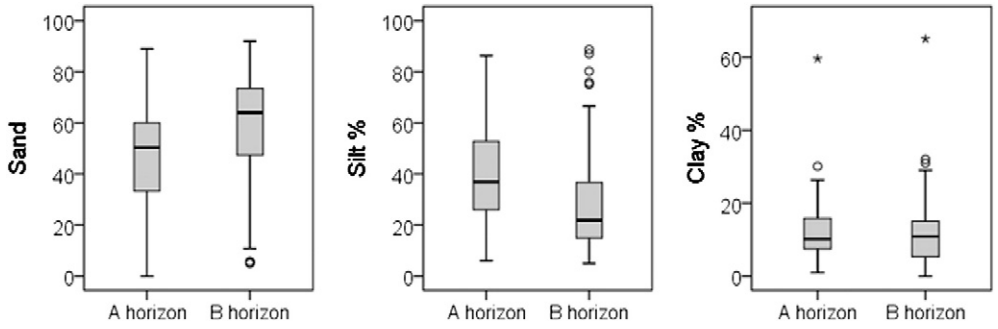

Fig. 4. Boxplots showing the relative abundance of sand, silt, and clay in A and B horizons of Uinta alpine soils, determined through sieving and hydrometer analysis.

Table 3
Results of grain size analysis with laser scattering.

Sample type	Statistic	Mean µm	Median µm	Mode µm	SD µm	cSand %	mSand %	fSand %	vfSand %	cSilt %	mSilt %	fSilt %	vfSilt %	Clay %
A horizons	Mean	105.9	50.7	155.5	130.6	4.1	10.5	9.5	10.9	13.3	15.3	14.4	14.0	8.2
	Median	86.9	31.9	72.2	127.0	1.4	6.8	8.0	9.2	13.0	14.7	13.1	12.9	6.7
	Max	377.1	391.5	1089.6	495.7	33.7	35.1	24.0	41.5	25.8	36.9	28.6	41.0	59.6
	Min	6.1	0.3	0.1	6.1	0.0	0.0	0.0	0.0	0.9	5.0	2.6	2.9	0.3
	Skewness	1.32	3.51	2.18	1.42	2.72	0.71	0.55	2.20	0.51	1.34	0.34	1.33	3.97
	Count	61	61	61	61	61	61	61	61	61	61	61	61	61
B horizons	Mean	129.7	82.1	187.3	144.2	6.8	14.2	9.6	5.8	8.2	13.0	14.9	15.5	12.0
	Median	103.0	18.8	245.9	150.9	2.8	14.4	9.1	5.4	8.5	12.9	12.2	14.3	9.2
	Max	467.1	466.0	628.3	329.0	45.7	42.2	19.5	11.0	14.9	27.8	36.6	31.8	65.0
	Min	12.0	0.2	0.1	33.2	0.0	0.1	2.3	1.6	1.8	2.0	2.5	3.9	0.0
	Skewness	1.73	2.10	0.64	0.66	2.38	0.65	0.34	0.23	−0.03	0.26	1.15	0.56	2.94
	Count	22	22	22	22	22	22	22	22	22	22	22	22	22
Fines in snow	Mean	88.8	42.3	57.0	114.2	3.4	3.3	7.9	22.3	19.1	14.9	14.3	12.7	2.1
	Median	60.2	38.7	72.2	55.7	0.0	1.4	7.5	18.7	18.8	15.0	13.2	12.9	2.3
	Max	293.4	84.6	83.1	398.2	24.1	15.2	15.0	41.5	25.8	21.9	25.0	23.8	4.4
	Min	30.0	14.2	9.5	37.1	0.0	0.1	3.1	11.4	12.4	10.4	6.1	4.0	0.3
	Skew	2.07	0.37	−1.00	1.81	2.36	1.72	1.27	0.87	0.33	0.78	0.39	0.18	0.24
	Count	14	14	14	14	14	14	14	14	14	14.0	14	14	14
Soil Near Snow	Mean	145.7	82.3	236.3	158.4	4.8	20.1	14.7	8.7	11.8	12.2	9.7	10.5	7.4
	Median	149.2	61.9	280.5	166.4	4.3	19.9	14.2	8.7	12.4	12.3	9.7	10.5	6.0
	Max	271.0	242.1	368.2	210.0	13.1	35.9	24.0	11.7	17.0	21.1	17.5	17.1	26.4
	Min	39.2	10.9	0.2	56.7	0.0	1.6	6.6	5.6	4.0	4.3	2.6	2.9	1.1
	Skew	0.47	1.41	−1.22	−1.04	0.92	0.08	0.43	0.09	−0.64	−0.01	0.01	−0.17	2.45
	Count	14	14	14	14	14	14	14	14	14	14.0	14	14	14
Lake sediments	Mean	18.3	9.4	11.5	24.6	0.0	0.2	1.1	4.4	12.6	18.2	19.4	22.0	22.1
	Median	17.6	9.7	10.8	22.7	0.0	0.0	0.3	3.7	13.7	17.6	19.4	21.1	22.7
	Max	40.7	22.3	18.6	54.6	0.0	1.5	5.6	11.5	21.4	27.9	24.7	31.1	38.8
	Min	6.1	3.5	7.2	8.1	0.0	0.0	0.0	0.0	2.6	9.4	15.9	11.0	4.3
	Skew	1.02	1.43	0.72	1.04	–	3.01	2.02	0.36	−0.71	0.24	0.41	0.01	−0.09
	Count	21	21	21	21	21	21	21	21	21	21	21	21	21

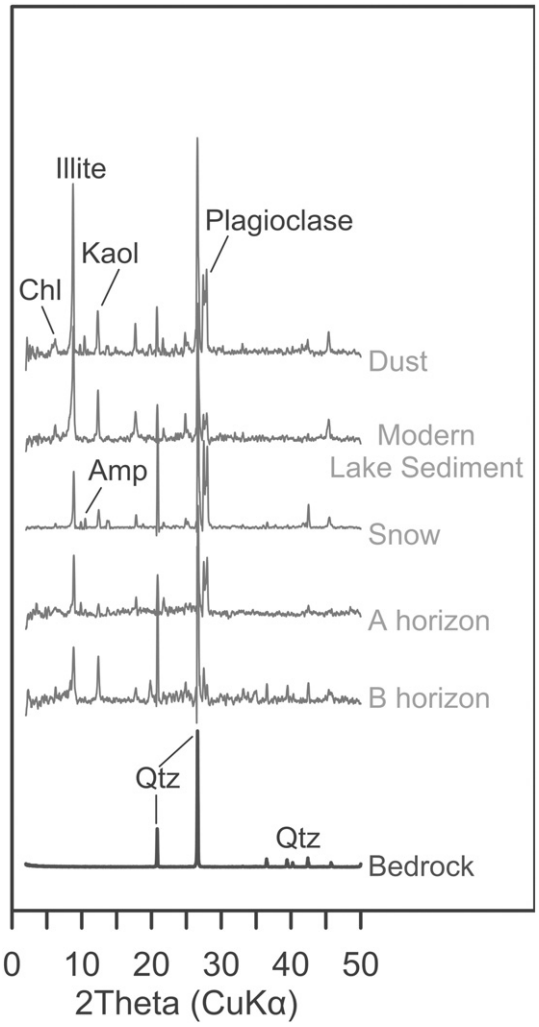

Fig. 5. X-ray diffraction (XRD) results for various sediment types considered in this study. Dust, modern lake sediment, fine material isolated from snow, and soils contain quartz, plagioclase, illite, kaolinite, amphibole, and trace amounts of chlorite. In contrast, only quartz is detectable in Uinta bedrock. X-ray patterns are presented with background removed and minor smoothing applied for clarity.

eolian inputs (Fig. 5). On the other hand, amphibole, which is also present in modern dust, was not detected in lake sediments. This suggests a lack of amphibole in the lake sediments, although it is also possible that trace amphibole was undetectable above the high background levels of amorphous material (likely diatoms) in these samples.

The water content of the most recently deposited sediment was extremely high (~95%) in all seven of the sampled lakes. As a result, the dry mass of the top-most sample from five of the lakes was too small for ICP-MS analysis; however, in the other two lakes the modern samples are enriched in Bi, Cu, Na, P, Zn, Cd, Sn, and Pb (Fig. 8). Enrichment of these elements relative to the sample from ~30 cm depth averages 1.8×, with the maximum enrichment (>4×) seen in Bi and Pb. Abundances of immobile elements are more variable in lake sediment samples; however, the majority overlap with the modern dust, and none overlap with Uinta bedrock (Fig. 6).

5. Discussion

5.1. Influence of dust on alpine pedogenesis

The data collected for this study demonstrate that soils in the alpine zone of the Uinta Mountains have been strongly influenced by dust deposition. The most visible consequence of long-term dust accretion is the layer of silt found at the surface of every soil profile (Fig. 2). Previous studies proposed that this sediment is a loess cap because of its grain-size, ubiquity, and consistent thickness over landforms of varying age (Bockheim and Koerner, 1997; Bockheim et al., 2000). The more extensive set of observations presented here supports this interpretation, confirming that the silt layer is present throughout the alpine zone with consistent thickness and properties. The grain-size distribution of soil A horizons strongly overlaps with that of modern dust, further suggesting that A horizons contain abundant eolian sediment. Bivariate plots of immobile elements indicate that the fine fraction of the A horizon is very similar to the modern dust, and is distinct from the underlying bedrock (Fig. 6). Additional evidence for the exotic origin of this material is provided by XRD analysis, which reveals the presence of plagioclase and amphibole in A horizons and modern dust, and a general lack of these minerals in Uinta bedrock (Fig. 5). Thus, eolian delivery of fine material sourced from outside the Uinta region is contributing to the formation of these A horizons. Exotic amphibole has also been noted in soils of the Wind River Range, ~200 km north of the Uintas (Fig. 1), and the expansive Green River Basin between the two mountain ranges has been proposed as a source for this mineral (Dahms, 1993).

The age of the silt remains uncertain; however, previous work has demonstrated that an undisturbed loess cap is present in soil profiles from within the centers of sorted stone polygons that were presumably active during the last glaciation (Munroe, 2007). Because any preexisting loess cap would have been cryoturbated into the soil profile when these polygons were active, accumulation of the loess must have occurred since the last deglaciation, ca. 15,000 years ago (Laabs et al., 2009). Considering the mean bulk density (0.95 g/cm^3), organic C content (10%), and silt content (57%) of A horizons in the alpine zone, the average rate of modern dust deposition (3.5 g/m^2/yr) could produce a loess cap ~15 cm thick in 15,000 years. This rough estimate does not take into account translocation of silt into the soil profile, loss of dust from the surface through erosion, or changes in the rate of dust delivery over time. Nonetheless, the agreement between this estimate and the measured thickness of loess (Fig. 3) is strong evidence that dust deposition has been a long-term process.

Lab analysis of physical and chemical properties underscores strong differences between A and B horizons in Uinta alpine soils. Many of these differences stem from the formation of these horizons in two different parent materials: silty dust for A horizons, and sandy congelifractate for B horizons. Mixing of these two parent materials is occurring, as evidenced by the appreciable amounts of silt in B horizons, and significant sand and sparse coarse fragments in A horizons (Tables 2 and 3). The presence of A2 horizons in many profiles may further reflect mixing of these two end member parent materials, as does the geochemical similarity between dust and the fine fraction of the B horizon. Even with mixing though, most properties of these horizons are distinct, with higher levels of organic matter and exchangeable cations in A horizons, and elevated bulk density in B horizons (Table 2). The pronounced textural discontinuity between the dust-derived A horizon and the underlying coarser B horizon likely impacts the downward percolation of water through these soils, possibly contributing to a seasonal water deficit in the subsoil (e.g. Doering and Reider, 1992). The significantly higher abundance of Ca in the loess cap, and in the modern dust (Table 4), may also contribute to buffering of soils (Bockheim et al., 2000). Overall, these results from the Uintas corroborate studies elsewhere in the Rocky Mountains documenting the important influence of long-term eolian deposition on the development of mountain soils (e.g. Lawrence et al., 2011, 2013; Muhs and Benedict, 2006).

5.2. Origin and significance of fine sediments in late-lying snowbanks

Field observations of snowbanks lingering in the alpine zone of the Uintas in late spring/early summer commonly reveal concentrations of dark colored, fine sediment on the snow surface. Given the recent focus on the influence of dust on snow albedo in the Rocky Mountains

Table 4
Mean elemental abundances.

Element	Units	Detection limit	Bedrock	Coarse dust	Fine dust	A horizons	B horizons	Snow	SNS[a]	Lake sediment
Ag	ppm	0.02	0.04	0.04	0.34	0.17	0.07	–	–	0.10
Al	%	0.01	1.65	2.42	6.94	7.45	9.57	5.30	8.26	9.15
As	ppm	1	38.50	21.80	13.50	10.57	10.26	3.33	9.36	7.33
Ba	ppm	1	61.25	197.64	706.30	642.14	645.16	444.11	678.64	818.78
Be	ppm	0.1	0.35	1.03	2.88	2.81	3.41	1.66	2.95	4.13
Bi	ppm	0.04	0.29	0.51	9.70	0.46	0.40	0.38	0.53	0.38
Ca	%	0.01	0.06	0.16	1.02	0.79	0.45	0.42	0.63	0.32
Cd	ppm	0.02	0.07	0.08	0.98	0.54	0.21	0.11	0.46	0.36
Ce	ppm	0.05	20.83	40.12	73.60	68.46	95.58	43.29	71.48	81.96
Co	ppm	0.1	3.53	4.66	11.17	11.60	13.70	7.13	12.69	17.77
Cr	ppm	1	14.00	21.36	42.60	34.14	41.95	14.44	25.91	47.83
Cs	ppm	5	–	8.00	7.40	8.00	7.89	–	6.50	10.50
Cu	ppm	0.5	10.68	35.65	314.85	98.41	39.97	92.18	23.54	89.87
Dy	ppm	0.05	–	0.75	3.79	3.05	3.47	1.80	3.21	4.52
Er	ppm	0.05	–	0.54	2.09	1.73	1.96	1.04	1.80	2.53
Eu	ppm	0.05	–	0.32	1.33	1.03	1.21	0.66	1.15	1.39
Fe	%	0.01	1.82	1.14	3.01	3.11	4.14	1.85	3.28	3.36
Ga	ppm	0.1	4.25	7.51	16.36	18.97	27.68	–	–	30.66
Gd	ppm	0.05	–	0.93	4.26	3.73	4.44	2.24	4.11	5.58
Hf	ppm	0.02	1.17	1.17	2.67	2.75	3.62	–	–	3.93
Ho	ppm	0.05	–	0.10	0.71	0.58	0.66	0.35	0.61	0.87
In	ppm	0.02	–	0.05	0.08	0.08	0.08	0.04	0.07	0.07
K	%	0.01	0.69	1.07	2.42	2.22	2.54	2.16	2.49	2.86
La	ppm	0.1	11.05	19.07	36.71	34.36	47.26	22.56	36.51	41.61
Li	ppm	1	5.75	10.36	49.20	54.00	59.89	25.33	54.45	43.30
Lu	ppm	0.01	0.06	0.10	0.31	0.27	0.32	0.18	0.28	0.43
Mg	%	0.01	0.13	0.28	1.09	0.95	1.05	0.57	0.97	0.94
Mn	ppm	2	117.50	76.73	491.80	511.43	472.00	168.00	558.18	189.48
Mo	ppm	0.05	1.69	0.26	1.46	1.53	1.58	–	–	1.80
Na	%	0.01	0.14	0.34	0.92	0.58	0.48	0.91	0.68	0.26
Nb	ppm	0.1	2.15	4.65	9.84	12.90	15.88	–	–	12.73
Nd	ppm	0.1	–	8.63	28.37	24.20	31.79	16.02	27.47	27.17
Ni	ppm	0.5	6.28	26.25	89.27	33.31	46.78	26.30	32.40	42.75
P	ppm	50	112.50	243.64	4044.00	1507.14	1229.47	388.89	1382.73	1645.65
Pb	ppm	0.5	7.90	19.20	85.04	47.36	31.60	15.83	34.34	44.17
Rb	ppm	0.2	18.68	44.70	116.46	132.43	143.47	91.48	135.82	124.52
S	%	0.01	0.01	0.04	0.02	0.13	0.08	0.03	0.10	0.14
Sb	ppm	0.05	0.36	0.94	1.67	1.20	1.00	–	–	0.91
Sc	ppm	0.1	1.50	3.60	9.17	11.17	15.45	–	–	17.60
Sm	ppm	2	–	1.28	5.34	4.59	5.85	2.93	5.24	5.88
Sn	ppm	0.3	0.55	2.26	16.97	7.89	5.17	4.10	2.50	4.33
Sr	ppm	0.5	38.88	41.45	180.40	136.71	128.78	120.48	139.82	94.01
Ta	ppm	0.05	0.12	0.45	0.65	1.03	1.31	–	–	1.08
Tb	ppm	0.05	0.16	0.26	0.72	0.62	0.74	0.32	0.59	1.03
Te	ppm	0.05	–	–	0.09	0.09	0.07	–	0.07	0.08
Th	ppm	0.2	3.25	7.24	11.46	12.69	19.52	8.92	14.83	21.77
Ti	%	0.01	0.08	0.11	0.32	0.31	0.40	0.27	0.34	0.26
Tl	ppm	0.02	0.08	0.24	0.75	0.71	0.88	0.55	0.79	0.74
U	ppm	0.05	0.84	1.57	3.07	3.16	4.34	2.04	3.44	6.39
V	ppm	2	21.25	20.82	62.70	66.00	93.00	34.22	68.55	82.30
W	ppm	0.1	0.15	0.42	1.74	2.03	2.20	–	–	1.80
Y	ppm	0.1	3.75	6.30	21.56	18.66	21.37	10.86	18.79	28.46
Yb	ppm	0.1	0.43	0.66	2.01	1.73	2.02	1.03	1.68	2.80
Zn	ppm	1	12.75	38.00	420.90	123.14	100.79	58.78	115.27	94.65
Zr	ppm	0.5	36.58	36.50	78.96	81.31	102.36	65.93	89.48	88.20

[a] Soil near snowbanks.

in general (e.g. Lawrence et al., 2010; Painter et al., 2010), and in northern Utah in particular (e.g. Carling et al., 2012; Reynolds et al., 2013; Steenburgh et al., 2012), it would be useful to clarify whether this material is allochthonous, or whether it was transported onto the snow from the surrounding land surface during the melt season when snowbanks become isolated from one another by expanding areas of tundra and bare ground.

Close inspection of the grain-size distribution of sediment isolated from the snow suggests that this material is a mixture of two end members, one that is silty and another that is coarser (Fig. 7). The simplest interpretation is that the silty material represents exotic dust, whereas the coarser sediment is derived from the unvegetated soil surface in the nivation zone around each snowbank. The SNS samples are generally sandier than A horizons elsewhere in the alpine zone because snowmelt winnows fines from the soil surface (Table 3). Results of XRD analysis indicate that both the snow and SNS samples contain amphibole, which is not present in local bedrock or soil B horizons (Fig. 5). Thus, both types of sediment are influenced by eolian delivery of allochthonous material. Bivariate plots support the idea that snow samples are a mixture; SNS samples plot in the same region as modern dust and A horizons, whereas snow samples plot along a mixing line between dust and Uinta bedrock, suggesting a combination of local and exotic sources (Fig. 6).

Because the snow samples were hand packed into Nalgene bottles, their original volumes are not known and the absolute concentration of dust in each sample cannot be determined. Instead, the relative abundance of exotic dust and locally derived material was estimated. This calculation was made by normalizing the abundance of very fine (2–7 μm) silt in each snow sample to the average very fine silt abundance (30%) in the modern dust, given that this is the most abundant

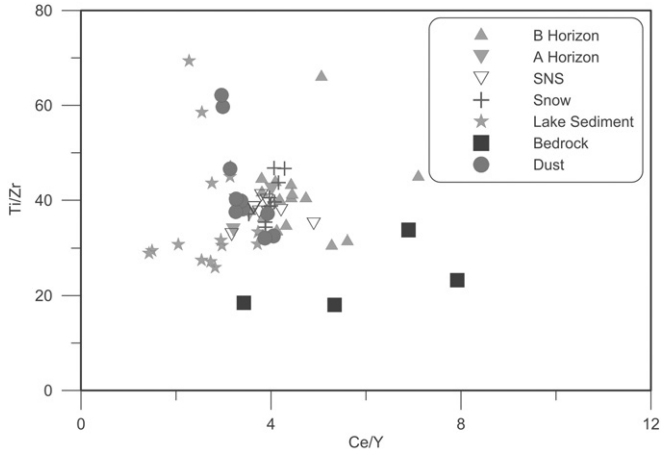

Fig. 6. Bivariate plot of the immobile elements Ce, Y, Zr, and Ti by weight in various sediment types considered in this study. None of the sediment samples overlaps with Uinta bedrock, but all of the sediment samples overlap with modern dust.

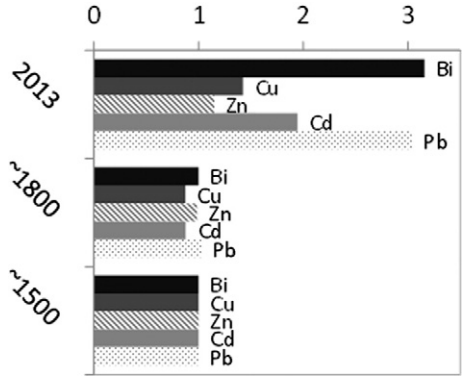

Fig. 8. Anthropogenic enrichment of several mining-related elements in the surface sediment of two lakes in the Uinta Mountains. Values are normalized to the bottom sample, assumed from ^{210}Pb depth-age models to have been deposited in the 16th century.

grain-size fraction in the allochthonous material. This approach reveals that exotic dust makes up 18 to 82% of the fine sediment in the 14 samples collected from snowbanks, with a mean of 47%. Snowbanks with the greatest proportion of exotic dust, relative to local material, tend to be located in two locations. Some are found on ridgecrests, where meltwater cannot carry sediment downslope onto the snow surface. Others are located on relatively steep slopes mantled by blocky scree. The coarse nature of this scree allows water to travel beneath late-lying snowbanks, rather than over them. In contrast, snowbanks with the smallest fraction of exotic dust tend to be located on slopes with less abundant rock cover. Meltwater in these settings can carry eroded material onto the snowbank during the late spring/early summer, diluting the amount of exotic dust that accumulated during the winter. This process might be expected to grow in importance through the melting season, as an increasing fraction of the surrounding landscape is uncovered. Future sampling efforts intended to isolate the eolian component from snow in alpine areas should target snowbanks on ridgecrests or steep blocky slopes, ideally early in the melt season before too much of the alpine zone is uncovered.

5.3. Lacustrine evidence for long-term dust deposition

The strong similarity between the grain-size distributions of the lake sediment samples and modern dust (Fig. 7) indicates that eolian sediment is accumulating in the lake basins. This conclusion is bolstered by the presence of plagioclase in lake sediment samples, compared with the general lack of this mineral in Uinta bedrock (Fig. 5). Bivariate plots of immobile elements further indicate that the fine fraction of the lake sediment samples is geochemically similar to modern dust, and distinct from the underlying bedrock (Fig. 6).

Because the overall grain-size distributions in the sampled lakes did not shift in consistent or dramatic ways during the time period represented by the cores, it appears that dust deposition is not a new process in the Uintas. Even given the uncertainty in the absolute ages for the middle (~15 cm) and bottom (~30 cm) samples from each core, the consistency of existing ^{210}Pb age models strongly suggests that these deeper samples represent sedimentation before European settlement. Thus, eolian delivery of fine material to the Uinta landscape appears to be an ongoing process that has operated over at least the latest part of the Holocene. This conclusion provides support for the inference that the ~18-cm thick loess cap in the alpine zone represents accretion of eolian dust throughout the post-glacial period.

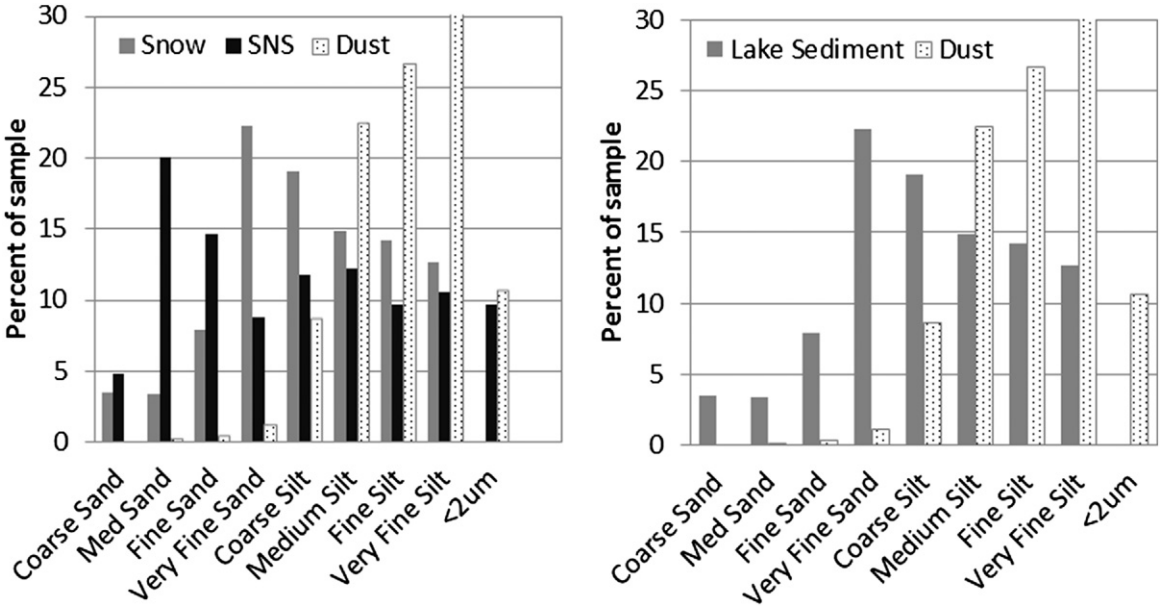

Fig. 7. Comparison of the grain-size distribution for snow, SNS, and dust samples (left), and for lake sediment and dust (right).

5.4. Recent anthropogenic changes in dust properties

One of the most striking observations about the geochemistry of the modern Uinta dust is its dramatic enrichment in elements associated with upwind mining and agriculture (Munroe, 2014). Analysis with ICP-MS reveals that Bi, Na, P, Zn, Sn, Cu, Cd, Ba, Ni, W, Sb, Pb, and Tl in Uinta dust are elevated 10× to >80× above their abundances in local bedrock. Many of these elements are also enriched in the surficial sediments considered in this study, although generally to lesser degrees (Table 4). For instance, Cu, which has a mean abundance of 315 ppm in modern dust samples, averages ~90 ppm in A horizon, snow, and lake sediment samples. In contrast, the abundance of Cu in B horizons is ~40 ppm, and in the local bedrock ~10 ppm (Table 4). The enrichment of these elements supports the conclusion that dust deposition is influencing the geochemistry of the Uinta alpine zone. Moreover, the notably higher abundances of Bi, Cu, Na, P, Zn, Cd, Sn, and Pb in the two samples of modern lake sediment that were large enough for ICP-MS analysis indicate that this enrichment is a modern phenomenon that was not operating before European settlement (Fig. 8). Thus, modern dust samples may be an imperfect analog for the dust that accumulated through most of the post-glacial period, at least with respect to these trace elements. Similar anthropogenic enrichment of metals in modern dust has been noted elsewhere in the western U.S., including in the Colorado Rockies (Lawrence et al., 2010; Neff et al., 2008), northern Utah (Reynolds et al., 2013), and elsewhere in the Uintas (Reynolds et al., 2010).

5.5. Implications

The results of this project have three broad implications for understanding dust systems in alpine settings beyond the Uinta Mountains. First, given the evidence that dust deposition is occurring in alpine zones throughout this region, models of soil function and evolution in alpine settings need to include potentially substantial effects of long-term dust deposition. Evidence from the Uintas indicates that this dust has accumulated during the post-glacial period to form a layer at the soil surface averaging ~20 cm thick. Furthermore, comparison of surface and subsurface horizons reveals that silty loess has translocated downward within the soil profile as well, mixing with the coarser, locally derived sediment. Aspects of soil fertility, rooting depth, stoniness, and other factors important for plant growth, water movement, and erodability may have changed over time as loess accumulated.

Second, the work presented here demonstrates that fine material at the surface of late-lying snowbanks contains a significant amount of locally derived sediment in addition to exotic dust. Models of the relationship between allochthonous dust, albedo, and snowmelt should consider the possible role of this local sediment, which might change in abundance under different fu climate scenarios.

Finally, the enrichment of various metals in the most recently deposited lake sediments is unequivocal evidence for anthropogenic impacts on the dust system in this region, supporting the work of Neff et al. (2008) in Colorado, and Reynolds et al. (2010) in the Uintas. Future work should be focused on the environmental geochemistry of alpine environments to determine whether increased delivery of these elements is negatively impacting alpine ecosystems.

6. Conclusion

The data collected for this project illuminate the effects and history of eolian dust deposition in the alpine zone of the Uinta Mountains. Soil profiles throughout the alpine zone are capped with a stone-poor layer rich in very fine silt that was produced by dust deposition over time. This unit contains mineral phases that are not present in the underlying bedrock, confirming an allochthonous origin. The grain-size distribution of this material, and its pattern of trace element abundances, matches the properties of modern dust samples collected between 2011 and 2013. The thickness of this layer is variable, but the mean of 18 cm is consistent with dust deposition at modern rates over the post-glacial period.

Fine clastic material sampled from the surface of late-lying snowbanks in the alpine zone is a mixture of exotic dust and sediment mobilized from the adjacent land surface by wind and flowing water. This fine material contains allochthonous minerals, and has a geochemical composition intermediate between modern dust and local bedrock. The abundance of exotic material relative to locally-derived sediment in the sampled snowbanks varies widely, from ~20% to >80%. Snowbanks on ridgecrests, and those overlying talus, are typically dominated by eolian dust; those in nivation hollows and on the lower portion of vegetated slopes tend to contain more local material.

Lake sediments that accumulated over the past few centuries have a grain-size distribution that overlaps with that of modern dust. Lake sediments also contain minerals not present in Uinta bedrock, and have a geochemical composition that matches modern dust samples and soil A horizons. Although depth-age models are not available for all the sampled lakes, the general consistence of sedimentation rates in the lakes that have been dated suggests that the deepest samples record sedimentation before European settlement of the surrounding lowland basins. Thus, dust deposition appears to have been a long-term process in the higher elevations of the Uintas.

Previous work has documented that modern dust accumulating in the Uintas is dramatically enriched in elements indicative of upwind mining and agricultural activity (Reynolds et al., 2010). The lake sediment cores collected for this project demonstrate that this enrichment is a recent development, corroborating other reports of significant anthropogenic contributions to eolian processes in the Rocky Mountain region.

Acknowledgments

Middlebury College provided support for this project through a Gladstone Excellence in Teaching award to J. Munroe, and Senior Work Supplements to E. Attwood and P. Quackenbush. The USFS provided logistical support and funding for some of the geochemical analyses. The authors thank Markus Egli, Thierry Adatte, and an anonymous reviewer for their comments which improved the manuscript.

References

Arimoto, R., 2001. Eolian dust and climate: relationships to sources, tropospheric chemistry, transport and deposition. Earth Sci. Rev. 54, 29–42.
Birkeland, P.W., Burke, R.M., Shroba, R.R., 1987. Holocene alpine soils in gneissic cirque deposits, Colorado Front Range. U.S. Geol. Surv. Bull. 1590, E1–E21.
Bockheim, J., Koerner, D., 1997. Pedogenesis in alpine ecosystems of the eastern Uinta Mountains, Utah, USA. Arct. Alp. Res. 29, 164–172.
Bockheim, J., Munroe, J., Douglass, D., Koerner, D., 2000. Soil development along an elevational gradient in the southeastern Uinta Mountains, Utah, USA. Catena 39, 169–185.
Bradley, W.H., 1936. Geomorphology of the North Flank of the Uinta Mountains. US Government Printing Office, Washington, DC.
Bradley, M.D., 1995. Timing of the Laramide rise of the Uinta Mountains, Utah and Colorado. Guideb. Wyo. Geol. Assoc. 1995, 31–44.
Brahney, J., Ballantyne, A., Sievers, C., Neff, J., 2013. Increasing Ca^{2+} deposition in the western US: the role of mineral aerosols. Aeolian Res. 10, 77–87.
Brahney, J., Ballantyne, A., Kociolek, P., Spaulding, S., Otu, M., Porwoll, T., Neff, J., 2014. Dust mediated transfer of phosphorus to alpine lake ecosystems of the Wind River Range, Wyoming, USA. Biogeochemistry 1–20.
Carling, G.T., Fernandez, D.P., Johnson, W.P., 2012. Dust-mediated loading of trace and major elements to Wasatch Mountain snowpack. Sci. Total Environ. 432, 65–77.
Christensen Jr., J.W., Jewell, P.W., 1998. Geochemical variations in an alpine lake and watershed underlain by siliciclastic bedrock, Uinta Mountains, Utah. Utah Geol. Assoc. Publ. 26, 59–69.
Dahms, D.E., 1993. Mineralogical evidence for eolian contribution to soils of late Quaternary moraines, Wind River Mountains, Wyoming, USA. Geoderma 59, 175–196.
Dahms, D.E., Rawlins, C.L., 1996. A two-year record of eolian sedimentation in the Wind River Range, Wyoming, U.S.A. Arct. Alp. Res. 28, 210–216.
Dehler, C.M., Porter, S.M., De Grey, L.D., Sprinkel, D.A., Brehm, A., 2007. The Neoproterozoic Uinta Mountain Group revisited; a synthesis of recent work on the Red Pine Shale and related undivided clastic strata, northeastern Utah, U.S.A. Spec. Publ. Soc. Sediment. Geol. 86, 151–166.

Dia, A., Chauvel, C., Bulourde, M., Gerard, M., 2006. Eolian contribution to soils on Mount Cameroon; isotopic and trace element records. Chem. Geol. 226, 232–252.
Doering, W.R., Reider, R.G., 1992. Soils of Cinnaber Park, Medicine Bow Mountains, Wyoming, USA: indicators of park origin and persistence. Arct. Alp. Res. 24 (1), 27–39 (USA).
Dymond, J., Biscaye, P.E., Rex, R.W., 1974. Eolian origin of mica in Hawaiian soils. Geol. Soc. Am. Bull. 85, 37–40.
Engelbrecht, J.P., Menéndez, I., Derbyshire, E., 2014. Sources of PM-2.5 impacting on Gran Canaria, Spain. Catena 112, 119–132.
Kurtz, A.C., Derry, L.A., Chadwick, O.A., 2001. Accretion of Asian dust to Hawaiian soils; isotopic, elemental, and mineral mass balances. Geochim. Cosmochim. Acta 65, 1971–1983.
Laabs, B.J.C., Refsnider, K.A., Munroe, J.S., Mickelson, D.M., Applegate, P.J., Singer, B.S., Caffee, M.W., 2009. Latest Pleistocene glacial chronology of the Uinta Mountains: support for moisture-driven asynchrony of the last deglaciation. Quat. Sci. Rev. 28, 1171–1187.
Lawrence, C.R., Neff, J.C., 2009. The contemporary physical and chemical flux of aeolian dust; a synthesis of direct measurements of dust deposition. Chem. Geol. 267, 46–63.
Lawrence, C.R., Painter, T.H., Landry, C.C., Neff, J.C., 2010. Contemporary geochemical composition and flux of aeolian dust to the San Juan Mountains, Colorado, United States. J. Geophys. Res. 115, G03007.
Lawrence, C.R., Neff, J.C., Farmer, G., 2011. The accretion of aeolian dust in soils of the San Juan Mountains, Colorado, USA. J. Geophys. Res. Earth Surf. 116, F02013.
Lawrence, C.R., Reynolds, R.L., Ketterer, M.E., Neff, J.C., 2013. Aeolian controls of soil geochemistry and weathering fluxes in high-elevation ecosystems of the Rocky Mountains, Colorado. Geochim. Cosmochim. Acta 107, 27–46.
Litaor, M.I., 1987. The influence of eolian dust on the genesis of alpine soils in the Front Range, Colorado. Soil Sci. Soc. Am. J. 51, 142–147.
Menéndez, I., Diaz-Hernandez, J., Mangas, J., Alonso, I., Sanchez-Soto, P., 2007. Airborne dust accumulation and soil development in the North-East sector of Gran Canaria (Canary Islands, Spain). J. Arid Environ. 71, 57–81.
Moser, K.A., Mordecai, J.S., Reynolds, R.L., Rosenbaum, J.G., Ketterer, M.E., 2010. Diatom changes in two Uinta mountain lakes, Utah, USA: responses to anthropogenic and natural atmospheric inputs. Hydrobiologia 648, 91–108.
Muhs, D.R., Benedict, J.B., 2006. Eolian additions to late Quaternary alpine soils, Indian Peaks Wilderness Area, Colorado Front Range. Arct. Antarct. Alp. Res. 38, 120–130.
Munroe, J.S., 2002. Timing of postglacial cirque reoccupation in the northern Uinta Mountains, northeastern Utah, USA. Arct. Antarct. Alp. Res. 34, 38–48.
Munroe, J.S., 2006. Investigating the spatial distribution of summit flats in the Uinta Mountains of northeastern Utah, USA. Geomorphology 75, 437–449.
Munroe, J.S., 2007. Properties of alpine soils associated with well-developed sorted polygons in the Uinta Mountains, Utah, USA. Arct. Antarct. Alp. Res. 39, 578–591.
Munroe, J.S., 2014. Properties of modern dust accumulating in the Uinta Mountains, Utah, USA, and implications for the regional dust system of the Rocky Mountains. Earth Surf. Process. Landf. http://dx.doi.org/10.1002/esp.3608.
Munroe, J.S., Laabs, B.J.C.,2009. Glacial geologic map of the Uinta Mountains area, Utah and Wyoming, 1:100,000.
Neff, J.C., Ballantyne, A.P., Farmer, G.L., Mahowald, N.M., Conroy, J.L., Landry, C.C., Overpeck, J.T., Painter, T.H., Lawrence, C.R., Reynolds, R.L., 2008. Increasing eolian dust deposition in the western United States linked to human activity. Nat. Geosci. 1, 189–195.
Painter, T.H., Barrett, A.P., Landry, C.C., Neff, J.C., Cassidy, M.P., Lawrence, C.R., McBride, K.E., Farmer, G.L., 2007. Impact of disturbed desert soils on duration of mountain snow cover. Geophys. Res. Lett. 34, L12502.
Painter, T.H., Deems, J.S., Belnap, J., Hamlet, A.F., Landry, C.C., Udall, B., 2010. Response of Colorado River runoff to dust radiative forcing in snow. Proc. Natl. Acad. Sci. 107, 17125–17130.
Psenner, R., 1999. Living in a dusty world: airborne dust as a key factor for alpine lakes. Water Air Soil Pollut. 112, 217–227.
Reheis, M.C., Budahn, J.R., Lamothe, P.J., Reynolds, R.L., 2009. Compositions of modern dust and surface sediments in the Desert Southwest, United States. J. Geophys. Res. Earth Surf. 114, F01028.
Reynolds, R.L., Mordecai, J.S., Rosenbaum, J.G., Ketterer, M.E., Walsh, M.K., Moser, K.A., 2010. Compositional changes in sediments of subalpine lakes, Uinta Mountains (Utah): evidence for the effects of human activity on atmospheric dust inputs. J. Paleolimnol. 44, 161–175.
Reynolds, R.L., Goldstein, H.L., Moskowitz, B.M., Bryant, A.C., Skiles, S.M., Kokaly, R.F., Flagg, C.B., Yauk, K., Berquó, T., Breit, G., 2013. Composition of dust deposited to snow cover in the Wasatch Range (Utah, USA): controls on radiative properties of snow cover and comparison to some dust-source sediments. Aeolian Res. http://dx.doi.org/10.106/j.aeolia.2013.08.001.
Sears, J., Graff, P., Holden, G., 1982. Tectonic evolution of lower Proterozoic rocks, Uinta Mountains, Utah and Colorado. Geol. Soc. Am. Bull. 93, 990–997.
Sow, M., Goossens, D., Rajot, J.L., 2006. Calibration of the MDCO dust collector and of four versions of the inverted frisbee dust deposition sampler. Geomorphology 82, 360–375.
Steenburgh, W.J., Massey, J.D., Painter, T.H., 2012. Episodic dust events of Utah's Wasatch front and adjoining region. J. Appl. Meteorol. Climatol. 51, 1654–1669.
Steltzer, H., Landry, C., Painter, T.H., Anderson, J., Ayres, E., 2009. Biological consequences of earlier snowmelt from desert dust deposition in alpine landscapes. Proc. Natl. Acad. Sci. 106, 11629–11634.
Thorn, C.E., Darmody, R.G., 1980. Contemporary eolian sediments in alpine zone, Colorado Front Range. Phys. Geogr. 1, 162–171.
Vandenberghe, J., 2013. Grain size of fine-grained windblown sediment: a powerful proxy for process identification. Earth Sci. Rev. 121, 18–30.